VOL. 10, NO. 11, JUNE 2015 ISSN 1819-6608
ARPN Journal of Engineering and Applied Sciences


www.arpnjournals.com

MRI BRAIN NUCLEI SEGMENTATION AND EVALUATION OF SEGMENTED NUCLEI WITH BET AND BSE

D. Selvaraj[1], R. Dhanasekaran[2] and D. Arul kumar[3]
[1]Department of Electronics and Communication Engineering, Sathyabama University, Chennai, India
[2]Department of Electrical and Electronics Engineering, Syed Ammal Engineering College, Ramanathapuram, India
[3]Department of Electronics and Communication Engineering, Panimalar Institute of Technology, Chennai, India
E-Mail: mails2selvaraj@yahoo.com

ABSTRACT

Segmentation of brain nuclei from MRI brain image is an essential preprocessing step towards a better segmentation in neuroimaging studies. Segmentation of brain tissues from brain nuclei in MR image is an important problem in biomedicine that involves a number of applications such as diagnosis, surgical planning, and brain disease studies like Alzheimer, schizophrenia. In the proposed method for brain nuclei segmentation, the brain surface is seen as a smooth manifold with relatively low curvature that separates brain from non-brain regions. Also, the brain cortex is seen as a distinct dark ring surrounding the brain tissues in the MR images. The proposed method is based on thresholds and morphological operators. The proposed method was tested on real MRI data obtained from Internet Brain Segmentation Repository (IBSR) and diagnostic centres. For validation, the proposed segmentation result is compared with standard skull stripping methods: Brain Extraction Tool (BET), Brain Surface Extractor (BSE). Performance was measured using the Jaccard Similarity Index (JSI) and Dice Similarity Score (DSS). The proposed method showed the best performance: JSI = 0.98, DSS = 0.979, Sensitivity = 0.979 and Specificity = 0.978 on brain web and JCC = 0.977, DSS = 0.966, Sensitivity = 0.98 and Specificity = 0.979 on diagnostic centre images.

Keywords: skull stripping, brain nuclei, morphological operator, MRI segmentation.

1. INTRODUCTION

Magnetic Resonance Imaging (MRI) is one of the frequently used diagnosing method for brain tumours in medical imaging. The major task in brain MRI segmentation is the classification of volumetric data into Gray Matter (GM), White Matter (WM), and Cerebrospinal Fluid (CSF). But, it is not easy as it sounds. There are some inbuilt difficulties regarding image segmentation; among them are radio frequency coil heterogeneity, brain tissue vulnerability, and other systematic artifacts. Several preprocessing steps have been presented to tackle some or all of these difficulties. The first processing step in the segmentation of brain tissues is skull stripping. The skull removed MR images are used for further classification of the brain tissues into normal (WM, GM, and CSF) and pathological tissues (tumour, cyst and edema).

Several skull stripping methods have been proposed by different researchers [1], [2]. These methods can be generally categorized into four types: morphological based, deformable surface based, atlas based and hybrid based [2]. As indicated in [1 - 2], the most commonly used skull stripping method is intensity thresholding followed by morphological operations to remove narrow connections. But, this method first uses operator input to determine certain threshold value, the region of interest or a seed for a region growing phase which is error prone as operator might not provide appropriate input and also it is time consuming.

In the proposed method for skull stripping, the middle brain slice from the brain sequence is selected and a binary mask is constructed using threshold value and morphological operators. Using the binary mask, the brain nuclei are extracted from the input image. The process is repeated for all the slices above and below the middle slice.

The remaining part of this paper is organized as follows. Section 2 represents the existing skull stripping methods. Section 3 represents the proposed skull stripping method. Validation of the proposed method is discussed in section 4. Simulation results are discussed in section 5. Finally the paper is concluded with the conclusion in section 6.

2. LITERATURE SURVEY

Brain Extraction Tool (BET) [4] uses deformable model to fit the brain's surface by the application of a set of locally adaptive model forces. The Brain Surface Extraction (BSE) tool [5] uses a combination of operations such as anisotropic diffusion filter, marr-hildreth edge detector and morphological operations to separate brain and non-brain tissues. The watershed algorithm [6] is an intensity based approach. But, it often produces over segmentation and it is sensitive to noise.

A hybrid method for skull stripping hybrid watershed algorithm (HWA) [7] works by combining the watershed techniques and a deformable surface model. This method first localizes a single white matter voxel in T1-w image and uses it to create a global minimum in the white matter before applying a watershed algorithm.

An automatic skull stripping algorithm [8] called the model based level set is based on active curve to remove the skull and intracranial tissues surrounding the brain in MR brain images. A skull stripping method [9] developed for coronal T1-weighted images based on

region growing aims to automatically detect 2 seed regions of the brain and non-brain by using the mask produced by morphological operations. Then the seed regions were expanded using 2D region growing algorithm. In [10], [11] a fully automatic brain extraction algorithm using diffusion, run length encoding and region labeling were developed for skull stripping in T2 weighted axial MR brain images.

Several other methods have been developed for skull stripping based on anisotropic diffusion filter and morphological processing [12], [13], seed growth and thresholding techniques [14], fuzzy ASM based [15] and deformable surface and tissue classification [16]. Most of these methods are applicable to T1 weighted MR brain images and does not extract the brain completely in all the slices. Moreover, none of these existing methods give satisfactory performance when evaluated for large-scale data set. It is due to the complexity of the human brain, varying image contrast properties, noise factor, variations in image orientations and types. There appears to be no single method that works well on all the three types of T1, T2 and PD weighted images.

3. THE PROPOSED FRAMEWORK

The steps involved in the proposed methodology for brain nuclei segmentation is shown in Figure 1. Initially, the middle brain slice is selected and a binary image is constructed using threshold value obtained from Otsu's threshold selection algorithm [3]. Then, morphological operators like opening and closing are used to eliminate obstacles and noise. Next, the largest connected component from binarized image is selected by considering the brain as the largest connected structure in the input image. Finally, the segmented brain nucleus is obtained by multiplying brain mask with input image. The above steps are described in detail in the following sections.

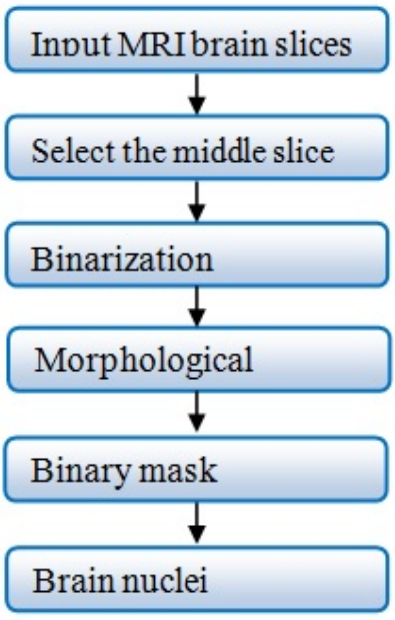

Figure-1. Proposed skull stripping framework.

a) Binarization

Binarization is the process of converting a grey level image into a binary image I (Equation 1). The binarization process involves examining the grey-level value of each pixel in the enhanced image with the global threshold 'Thres',

- If the pixel value (i, j) of the original image is lower than threshold, pixel (i, j) of binary image is black (value 0);
- If the pixel value (i, j) of the original image is higher than threshold, pixel (i, j) of binary image is white (value 1).

$$I = \begin{cases} \text{imbinary}(i,\ j) = 0;\ \text{if } I(i,j) < \text{Thres} \\ \text{imbinary}(i,j) = 1; \text{otherwise} \end{cases} \quad (1)$$

Otsu's method is the commonly used thresholding technique. It is simple and effective to implement. Otsu's thresholding technique is based on a discriminant analysis which partitions the image into two classes C_1 and C_2 at grey levels 'k' such that C_1 = { 0,1,2,3,…, k} and C_2 = { k+1, k+2,…, L-1} where, 'L' is the total number of grey levels of the image. Let 'n' be the total number of pixels in the given image and 'n_i' be the number of pixels at the i^{th} grey level. The probability of occurrence of grey level is defined as (Equation 2), where, 'C_1' and 'C_2' are two classes representing the ROI and the background. The probabilities of classes C_1 and C_2 are given by Equation 3 and Equation 4.

$$P_i = \frac{n_i}{n} \quad (2)$$

$$P_1(k) = \sum_{i=0}^{k} P_i \quad (3)$$

$$P_2(k) = \sum_{i=k+1}^{L-1} P_i = 1 - P_1(k) \quad (4)$$

The mean intensity values of these two classes C_1 and C_2 are given by Equation 5 to Equation 7.

$$m_1(k) = \sum_{i=0}^{k} i.P(i/C_1) \quad (5)$$

$$m_1(k) = \frac{1}{P_1(k)} \sum_{i=0}^{k} i.P_i \quad (6)$$

$$\text{Similarly, } m_2(k) = \frac{1}{P_2(k)} \sum_{i=k+1}^{L-1} i.P_i \quad (7)$$

Where, m_1 (k) and m_2 (k) are object's center grey and background's center grey. The cumulative (average intensity) up to level 'k' is given by Equation 8.

$$m(k) = \sum_{i=0}^{k} i.P_i \quad (8)$$

The total mean of the whole image is defined as (Equation 9),

$$m_G = \sum_{i=0}^{L-1} i.P_i \quad (9)$$

Let σ_B^2 and σ_T^2 be the between-class variance and total variance. An optimal threshold K* (Equation 10) can be obtained by maximizing the between-class variance.

$$K^* = Arg\left\{\max_{0<k\le L-1}\left(\frac{\sigma_B^2}{\sigma_T^2}\right)\right\} \quad (10)$$

The between-class variance σ_B^2 and the total variance σ_T^2 are defined as (Equation 11 and Equation 12),

$$\sigma_B^2 = P_1(m_1 - m_G)^2 + P_2(m_2 - m_G)^2 \quad (11)$$

$$\sigma_T^2 = \sum_{i=0}^{L-1} (i - m_G)^2.P_i \quad (12)$$

An equivalent and simpler formula for obtaining threshold K* is given as in Equation 13,

$$K^* = \max_{0\le k\le L} \left\{P_0(m_0 - m_T)^2 + P(m_1 - m_T)^2\right\} \quad (13)$$

Algorithm

Step-1: Compute probabilities of each intensity level

Step-2: Compute for various thresholds T = 1, 2, ….. , max intensity and i) upgrade P_i and m_i ii) Compute σ_B^2 (k)

Step-3: Select threshold value having max σ_B^2 (k)

The input MRI brain image in all the three planes (transverse, sagittal, and coronal) are shown in Figure-2 (a to c) and the binarized images obtained after applying Otsu's thresholding are shown in Figure-3 (a to c).

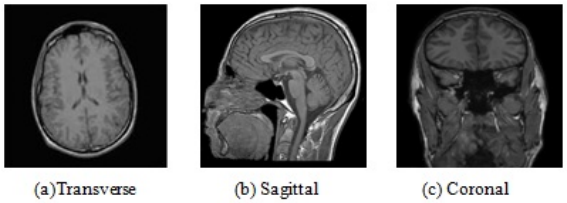

Figure-2. Input MRI brain images.

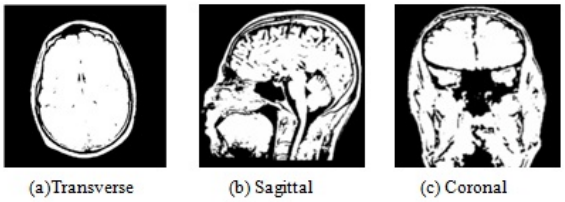

Figure-3. Binarized input MRI brain images.

b) Morphological operations

The morphological operators are then applied on the binarized image. Elimination of any obstacles and noise from the image is the primary function of the morphological operators. The morphological operators, namely opening and closing are used in the proposed method. White pixels are considered as foreground region and black pixels are considered as background region.

Closing operation: A closing operation consists of a dilation followed by erosion with the same structuring element S. A closing operation closes small holes in objects and fills narrow gaps in or between connected components. It is represented as (Equation 14):

$$I \bullet S = (I \oplus S) \ominus S \quad (14)$$

The syntax used in MATLAB is I' = imclose (I, S). Implementation of closing operator needs 2 processing steps: Binary erosion and dilation.

Erosion operation: Erosion operation on an image I containing labels 0 and 1, with a structuring element S, changes the value of pixel i in I from 1 to 0, if the result of convolving S with I, centered at 'i', is less than some predetermined value. This value is set to be the area of S, which is basically the number of pixels that are 1 in the structuring element itself.

The structuring element (also known as the erosion kernel) determines the details of how particular erosion thins boundaries. The syntax used in MATLAB is I' = imerode (I, S). Erosion operation makes the areas of foreground pixels shrink in size by eliminating irrelevant detail from binary image. This is carried by moving a disk structuring element S on the binary image I (Equation 15).

$$I \ominus S = \{(i, j): S_{ij} \subseteq I\} \quad (15)$$

This equation indicates that the erosion of I by S is the set of all image pixel points (i, j) such that S, translated by (i, j), is contained in I.

Algorithm: Calculation of binary erosion

1. Read the binary image as B_{img}.
2. Choose the size of the structuring element as M x N
3. Do the following steps in each pixel of the B_{img}.
   i. Get the pixel $B_{img}(i,j)$ and select the neighbouring pixels of $B_{img}(i,j)$ using S value of MxN and take it as W(i, j).
      W (i, j) = B_{img} [i-M: i+M, j-N: j+N]
   ii. Find the minimum value of W(i, j) and store the minimum value in E_{img}.
      E_{img} = min (W(i, j))
   iii. Replace all the pixel values of the window by E_{img}

$W(i, j) = E_{img}$

Dilation operation: Dual to erosion, a dilation operation on an image I' containing labels 0 and 1, with a structuring element S, changes the value of pixel 'i' in I from 0 to 1, if the result of convolving S with I', centered at 'i', is above some predefined value. This value is set to be zero.

The structuring element (also known as dilation kernel) determines the details of how a particular dilation grows boundaries in an image. Since the brain is an oval shaped image, a disk shaped structuring element as shown in Figure-4 is chosen in the convolution process. The structuring element used in almost all process is a 3x3 disk shaped. The syntax used in MATLAB is I" = imdilate (I', S).

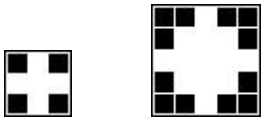

Figure-4. Disk shape structuring elements.

Dilation operation makes the areas of foreground pixels grow in size, while reducing the holes with in those regions. This is carried by moving a disk structuring element S on the binary image I' (Equation 16).

$$I \oplus S = \{(i, j): Sij \cap I \neq \phi\} \quad (16)$$

Where, Φ is the empty set. The dilation of I' by S is the set of all image pixel points, (i, j), such that S and I' overlap by at least one element.

Algorithm: Calculation of binary dilation

1. Take the W(i, j) values as input for dilation process.
2. Choose the same structuring element as MxN.
3. Do the following steps in each pixel of W(i, j)
   i. Get the pixel of W(i, j) and select the neighbouring pixels of W(i, j) using S Value of MxN and take it as V(i, j).
      V(i, j) = W(i, j) [i-M: i+M, j-N: j+N]
   ii. Find the maximum value of D_{img} = max(V(i, j))
   iii. Replace all pixel values of the window by D_{img}
      $V(i, j) = D_{img}$

Thus the closing operation closes small holes in the binary image, and fills narrow gaps in or between the connected components.

Opening: An opening operation consists of erosion followed by dilation with the same structuring element S. As coarse description of its functionality this operation removes components smaller than S and opens thin, elongated bridge between larger components. The syntax in MATLAB is I" = imopen (I, S). It is represented as Equation 17:

$$IoS = (I \Theta S) \oplus S \quad (17)$$

The fine MRI brain images (transverse, sagittal, and coronal) obtained after applying morphological operators are shown in Figure-5 (a to c).

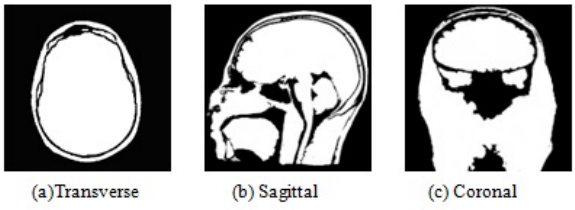

Figure-5. Fine MRI brain images.

c) Largest connected component selection

Binarization on brain MR images classifies the image into background and foreground leaving the foreground into a number of connected components. Connected component labeling is used to detect connected regions in the binary images. It scans an image pixel-by-pixel (from top to bottom and left to right) and groups its pixels into components based on pixel connectivity, that is, all pixels in a connected component share similar pixel intensity values and are in some way connected with each other. Once all groups have been determined, each pixel is labeled with a grey level or a colour (colour labeling) according to the component it was assigned.

Connected component labeling works on binary or grey level images and different measures of connectivity are possible. However, for the proposed framework binary input images and 8-connectivity are considered. The connected components labeling operator scans the image by moving along a row until it comes to a point p (where p denotes the pixel to be labeled at any stage in the scanning process) for which value V={1}. When this is true, it examines the four neighbours of p which have already been encountered in the scan (i.e. the neighbours (i) to the left of p, (ii) above it, and (iii) the two upper diagonal terms). Based on this information, the labeling of p occurs as follows:

- If all four neighbours are 0, assign a new label to p, else
- If only one neighbour has V={1}, assign its label to p, else
- If more than one of the neighbours have V= {1}, assign one of the labels to p and make a note of the equivalences.

After completing the scan, the equivalent label pairs are sorted into equivalence classes and a unique label is assigned to each class. As a final step, a second scan is made through the image, during which each label is replaced by the label assigned to its equivalence classes. Subsequently, the process results with a brain mask and stripped skull as shown in Figure-6. (a to f).

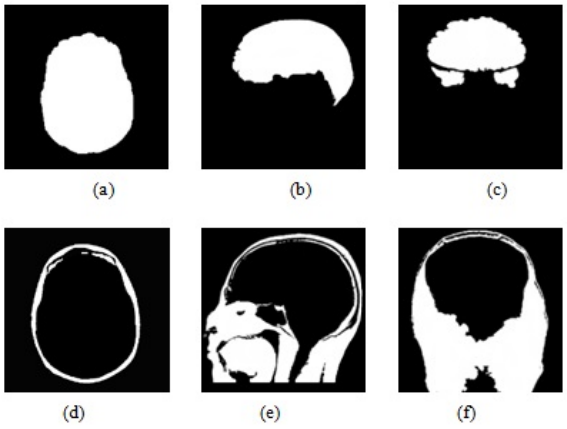

Figure-6. Brain mask and stripped skull images: (a), (b), (c) Brain mask and (d), (e), (f) Stripped skull.

d) Brain extraction

The brain is extracted by performing bitwise multiplication operation between the original image, Figure-2 (a to c), with the binary mask, Figure-6 (a to c). This process also removes background noise and other non brain artifacts. Thus the segmented brain nuclei image is as shown in Figure-7 (a to c).

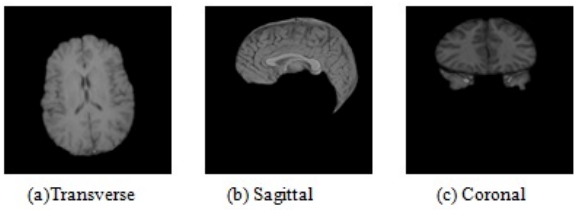

Figure-7. Segmented brain nuclei images.

4. PERFORMANCE VALIDATION METRICS

The performance of the proposed brain nuclei segmentation method is validated using the most commonly used validation metrics in the literature [17-20] which includes: Jaccard Similarity Index (JSI) [21], Dice Similarity Score (DSS) [22], specificity and sensitivity [23]. Validation is performed by comparing the proposed method's output with that obtained from manually segmented image. Let O_{S1} be the output obtained from manually segmented image and O_{S2} be the output result of the proposed method. JSI for the two sets is defined as the size of intersection of the two sets divided by the size of their union as given in Equation (18). A JSI value of 1 indicates a perfect agreement between the two sets.

$$JSI = \frac{|O_{S1} \cap O_{S2}|}{|O_{S1} \cup O_{S2}|} \quad (18)$$

DSS is defined as the size of intersection of the two sets divided by their average size as shown in Equation (19).

$$DSS = \frac{|O_{S1} \cap O_{S2}|}{\frac{1}{2}(|O_{S1} + O_{S2}|)} \quad (19)$$

Both JSI and DSS score measure the degree of overlap between O_{S1} and O_{S2}. The evaluation of brain abnormality detection in different images is carried out using the following metrics namely Sensitivity (SE), Specificity (SP), as given in Equations (20) and (21). In order to find these metrics, some of the terms like True Positive (TP), True Negative (TN), False Negative (FN), and False Positive (FP) are calculated based on the definitions given in Table-1.

$$SE = \frac{TP}{TP + FN} \quad (20)$$

$$SP = \frac{TN}{TN + FP} \quad (21)$$

SE is the proportion of TPs that are correctly identified by a diagnostic test. It shows how good the test is at detecting a disease. SP is the proportion of the TNs correctly identified by a diagnostic test. It suggests how good the test is at identifying normal (negative) condition.

Table-1. Defining the Terms TP, FP, FN, TN.

Experimental outcome	**Condition as determined by the standard of truth**		**Row total**
	Positive	Negative	
Positive Negative	TP FN	FP TN	TP+FP FN + TN
Column total	TP+FN	FP+TN	TP+TN+FP+FN

5. SIMULATION RESULTS

In this section, the simulation results are presented. Sample normal and abnormal brain MR images collected from IBSR, Diagnostic centres (Barnard Institute of radiology, Bharat scans and Sri Ramachandra diagnostic centre are shown in Figures-8(a), 9(a) and 10(a). After obtaining input MR brain images, the first step is to select the middle slice and segment the brain nuclei from it. The procedure is repeated for all the slices above and below the middle slices.

The efficiency and precision of skull stripping stage is highly important since subsequent stages in the pipeline of the tumour segmentation, use the output of this stage. The skull stripping method is tested on IBSR and diagnostic centre datasets. Figure-8(c), Figure-9(c) and Figure-10(c) show the segmented brain nuclei images of different patients with and without tumour.

a) Skull stripping performance measure

After obtaining input MR brain images, the first step is to remove non-brain tissues such as skull and scalp from MRI scans using the technique outlined in section III. Figure-10 shows the segmented brain nuclei images of a patient. In Figure-8 and Figure-9, the segmented brain nuclei images obtained using proposed method are compared with those obtained through BSE and in Figure 10, the skull stripped images of a patient for one full dataset is compared with BET.

JSI and DSS are used to measure the matching percentage of the proposed method with manual segmentation by overlapping these two methods. If both the methods are perfectly overlapping then the score will be '1' and the score will be '0' if there is no overlap between these two methods.

Sensitivity measures how well the performance of skull stripping method is in avoiding removal of brain tissues together with non-brain tissues. On the other hand, specificity measures how well the performance of the method on not wrongly classifying non-brain tissues as brain tissues.

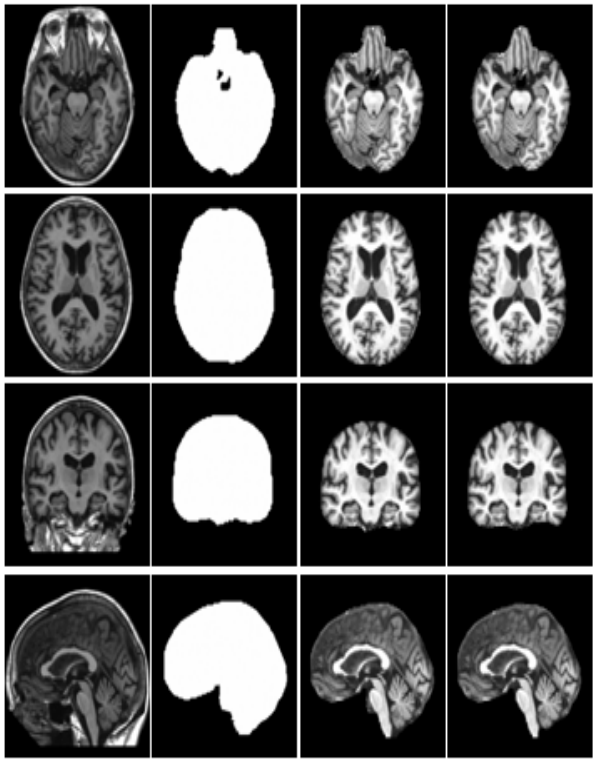

Figure-8. Segmented brain nuclei of normal brain images: a) Input brain MRI, b) Brain mask, c) Segmented brain nuclei by proposed method and d) Segmented brain nuclei by BSE.

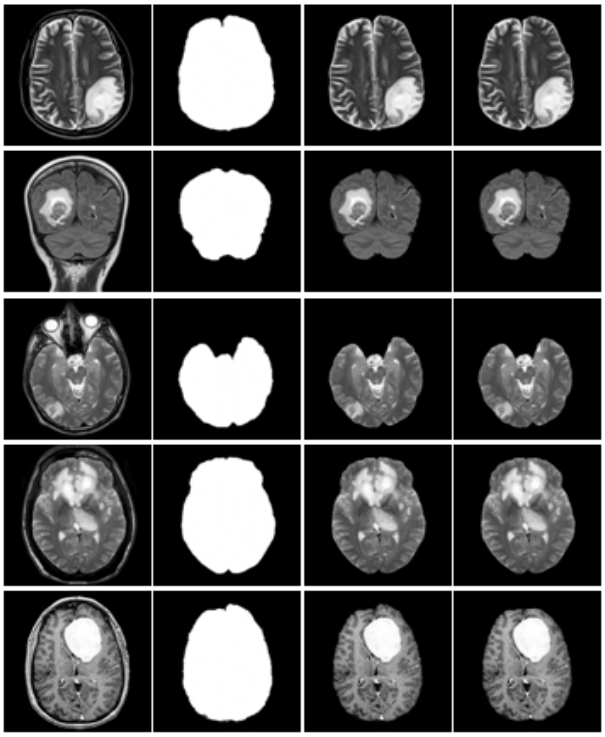

Figure-9. Segmented brain nuclei of abnormal brain MR images: a) Input brain MRI, b) Brain mask, c) Segmented brain nuclei by proposed method and d) Segmented brain nuclei by BSE.

Table-2. Brain nuclei extraction algorithm performance.

Performance measure		JSI	DSS	SE	SP	Time (sec)
BET	Dataset 1	0.84	0.89	0.90	0.94	22
	Dataset 2	0.87	0.92	0.93	0.88	34
BSE	Dataset 1	0.92	0.94	0.97	0.97	112
	Dataset 2	0.96	0.92	0.99	0.97	143
PROPOSED	Dataset 1	0.977	0.979	0.978	0.978	164
	Dataset 2	0.966	0.959	0.980	0.979	151

Table-3. Mean and SD value of JSI, DSS, SE and SP of proposed method.

Image		JSI	DSS	SE	SP
Mean	Dataset 1	0.977	0.979	0.978	0.978
	Dataset 2	0.966	0.959	0.980	0.979
	Dataset 3	0.978	0.956	0.966	0.968
SD	Dataset 1	0.0219	0.0266	0.0194	0.0269
	Dataset 2	0.0368	0.0345	0.0313	0.0429
	Dataset 3	0.0222	0.025	0.02	0.028

Larger value of SE indicates greater accuracy of the segmentation method. But, in case the skull stripping technique includes non-brain tissues in the final result rather than avoiding them, SE remains high. So, SE has to be coupled along with specificity to measure the accuracy of the skull stripping method.

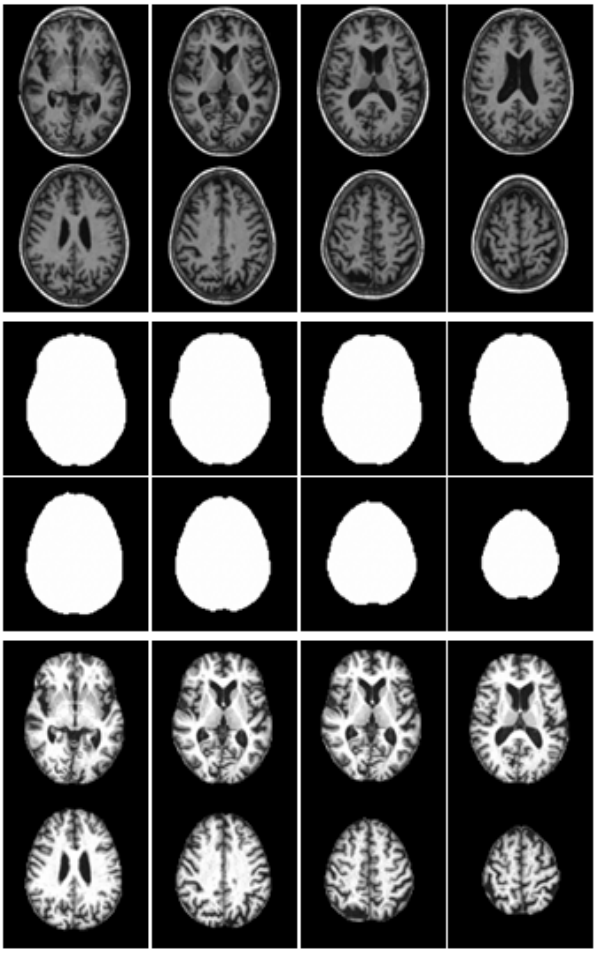

Figure-10. Skull stripped brain MR images of a patient for one full data sequence in transverse plane by BET.

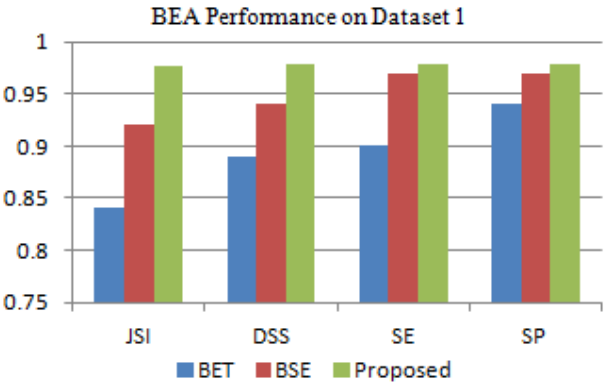

Figure-11. BEA performance on dataset 1 (Normal Images).

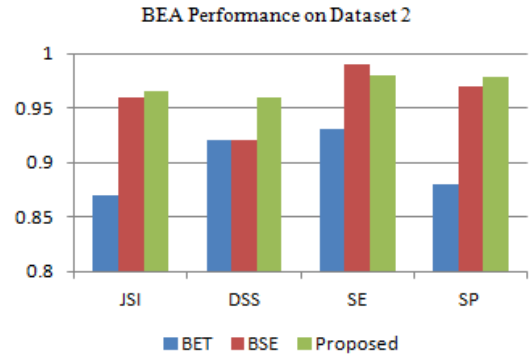

Figure-12. BEA performance on dataset 2 (Abnormal images).

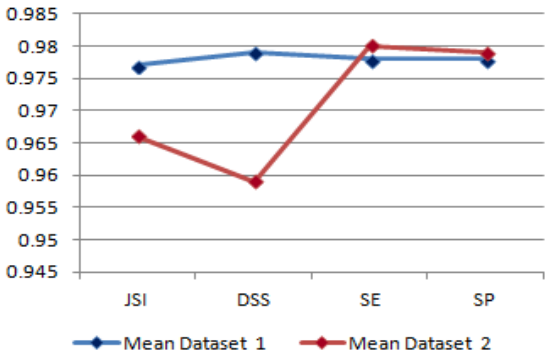

Figure-13. Mean value of JSI, DSS, SE and SP of proposed method.

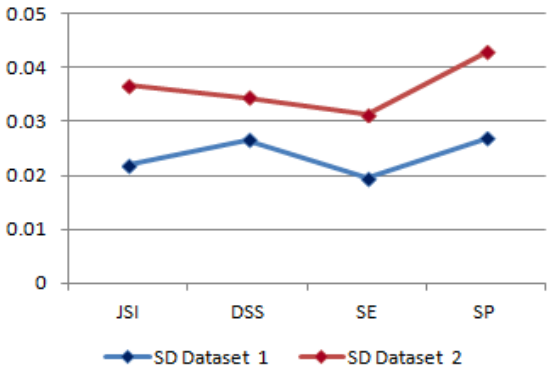

Figure-14. SD value of JSI, DSS, SE and SP of proposed method.

6. CONCLUSIONS

In this paper, a full automatic method for brain nuclei segmentation has been proposed and it is validated with two standard methods. From Tables-2 and 3, it can be observed that the skull stripping results are at an acceptable level, even to datasets where there is weak connection between brain tissues and darker intensities at the brain boundary. It can also be observed that the SE of the proposed method is on average, well above 98%.

Having higher SE is more important to avoid removal of brain tissues, which is critical for accuracy of subsequent stages.

Qualitatively Figures-8 to 10 show the result of skull stripping by the proposed method on IBSR and diagnostic centre datasets (patient1 and patient2) respectively. Mean and SD value of JSI, DSS, SE and SP of proposed method is shown in Figure-13 and Figure-14 and the comparison of JSI, DSS, SE and SP value of BET, BSE and proposed method is shown in Figure-11 and Figure-12. In this paper, the obtained results are at an acceptable level. In future, the features can be extracted from the brain nuclei to feed as input to a classifier to classify the input image as normal or abnormal.

REFERENCES

[1] E. H. Rubin *et al.* 1998. "A prospective study of cognitive function and onset of dementia in cognitively healthy elders", Archives of Neurology, Vol. 55, pp. 395-401.

[2] F. Segonne *et al.* 2004. "A hybrid approach to the skull stripping problem in MRI", Neuroimage, Vol. 22, No. 3, pp. 1060-1075.

[3] N. Otsu. 1979. "A threshold Selection Method from Gray-Level Histograms", IEEE Transactions on Systems, Man, and Cybernetics, Vol. 9, No.1, pp. 62-66.

[4] S. M. Smith. 2002. "Fast Robust Automated Brain Extraction," Human Brain Mapping, Vol.17, pp. 143-155.

[5] D. W. Shattuck, S. R. Sandor-Leahy, K. A. Schaper, D. A. Rottenberg and R. M. Leahy. 2001. "Magnetic Resonance Image Tissue Classification using a Partial Volume Model," Neuroimage, Vol. 13, pp. 856-876.

[6] H. Hahn and H. O. Peitgen. 2000. "The Skull Stripping Problem in MRI Solved by Single 3D Watershed Transform," Proc. of Medical Image Computing and Computer Assisted Intervention (MICCAI), LNCS, Vol.1935, pp. 134-143.

[7] S. Sandor and R. Leahy. 1997. "Surface-based labeling of cortical anatomy using a deformable database", IEEE Trans. Med. Imag., Vol. 16, pp: 41-54.

[8] A. H. Zhuang, D. J. Valentino and A. W. Toga. 2006. "Skull Stripping Magnetic Resonance Images using a Model-based Level Sets," NeuroImge, Vol. 32, No. 1, pp. 79-92.

[9] G. J. Park and C. Lee. 2009. "Skull Stripping Based on Region Growing for Magnetic Resonance Images," Neuroimage, Vol. 47, No. 4, pp. 1394-1407.

[10] K. Somasundaram and T. Kalaiselvi. 2010. "Fully Automatic Brain Extraction Algorithm for Axial T2-Weighted Magnetic Resonance Images," Computers in Biology and Medicine, Vol. 40, No. 10, pp. 811-822.

[11] T. Kalaiselvi. 2010. "Development of Fully Automatic Brain Extraction Methods for Magnetic Resonance Imaging (MRI) Head Scans and Detection of Abnormality in Brain, Ph.D. Thesis, Gandhigram Rural Institute – Deemed University, Gandhigram, India.

[12] J. Gao, and M. Xie. 2009. "Skull Stripping MR Brain Images using Anisotropic Diffusion Filtering and Morphological Processing," International Symposium on Computer Network and Multimedia Technology, Wuhan, Vol. 1. pp. 1-4.

[13] W. Zhao, M. Xie, J. Gao and T. Li. 2010. "A Modified Skull Stripping Method Based on Morphological Processing," Second International Conference on Computer Modeling and Simulation, Sanya, Hanna, Vol.1, pp. 159-163.

[14] K. J. Shanthi, and M. Sasikumar. 2007. "Skull Stripping and Automatic Segmentation of Brain MRI using Seed Growth and Threshold Techniques," International Conference on Intelligent and Advanced Systems, Kuala Lumpur, Vol.1, pp. 422-426.

[15] S. Kobashi, F. Y. Moto, M. D. Ogawa, K. Ando, R. Ishikura, S. H. Kando and Y. Katy. 2007. "Fuzzy-ASM Based Automated Skull Stripping Method from Infantile Brain MR Images," IEEE International Conference on Granular Computing, San Jose, California, Vol.1, pp. 632-635.

[16] X. Tao and C. M. Chang. 2010. "A Skull Stripping Method using Deformable Surface and Tissue Classification," Proc. SPIE, Vol. 7, pp. 623.

[17] W. Michael *et al.* 2008. "A Discriminative Model-Constrained Graph Cuts Approach to Fully Automated Pediatric Brain Tumor Segmentation in 3-D MRI", Lecture Notes in Computer Science, Medical Image Computing and Computer-Assisted Intervention –MICCAI 2008 , Vol. 5241, pp. 67-75.

[18] N. Gordillo, E. Montseny, P. Sobrevilla. 2010. "A New Fuzzy Approach to Brain Tumor Segmentation, Fuzzy Systems (FUZZ)", IEEE International Conference, 2010, pp.1-8.

[19] K. Kishore Reddy *et al.* 2012. "Confidence Guided Enhancing Brain Tumor Segmentation in Multi-Parametric MRI", 9th IEEE International Symposium on Biomedical Imaging, May, pp. 366-369.

[20] R. Nilanjan, G. Russell and M. Albert. 2008. "Using Symmetry to Detect Abnormalities in Brain MRI", Computer Society of India Communication, Vol. 31, No. 19, pp. 7-10.

[21] P. Jaccard. 1912. "The distribution of the flora in the alpine zone", The new phytologist, Vol.11, No.2, pp.37-50.

[22] L. R. Dice. 1945. "Measures of the Amount of Ecological Association between Species", Ecology, Vol. 26, No. 3, pp. 297-302.

[23] S. S. Coughlin and L. W. Pickle. 1992. "Sensitivity and Specificity-Like Measures of the Validity of a Diagnostic Test that are Corrected for Chance Agreement", Epidemiology, Vol. 3, No. 2, pp. 178-181.